Colloid Polym Sci (2004) 282: 461–467
DOI 10.1007/s00396-003-0969-z

ORIGINAL CONTRIBUTION

Y. Hayami
H. Sakamoto

Surface crystallization and phase transitions of the adsorbed film of $F(CF_2)_{12}(CH_2)_{16}H$ at the surface of liquid tetradecane

Received: 3 March 2003
Accepted: 20 June 2003
Published online: 17 September 2003

Y. Hayami (✉)
Department of Human Life Science,
Chikushi Jogakuen Junior College,
Dazaifu, 818–0192 Fukuoka, Japan
E-mail: hayami@chikushi-u.ac.jp
Tel.: +81-92925-3511
Fax: +81-92928-6253

H. Sakamoto
Kyushu Institute of Design,
815–8540 Fukuoka, Japan

Abstract The interaction between a long chain alkane, tetradecane (abbreviated H_{14}), molecule and a semi-fluorinated alkane, 1-perfluorododecyl-hexadecane $F(CF_2)_{12}(CH_2)_{16}H$ (abbreviated $F_{12}H_{16}$), molecule at the air/ H_{14} solution interface was studied by measuring the surface tension of the H_{14} solutions of $F_{12}H_{16}$ as a function of temperature and bulk concentration under atmospheric pressure. Pure liquid H_{14} freezes without forming a condensed film at its surface. Nevertheless, a very small amount of $F_{12}H_{16}$ initiates the surface freezing of H_{14}. In contrast to the $F_{12}H_{16}$-hexadecane (abbreviated H_{16}) system, the condensed monolayer of H_{14} has a finite solubility of $F_{12}H_{16}$ in the $F_{12}H_{16}$-H_{14} system. By further increasing the bulk concentration of $F_{12}H_{16}$, the F_{12} chains of the $F_{12}H_{16}$ molecules form the other closely packed condensed state. Hence, as in the case of the H_{16} system, the H_{14} system also exhibits a surface hetero-azeotrope behavior in the lower temperature region. Below the surface hetero-azeotropic point, the condensed H_{14} monolayer containing a small amount of $F_{12}H_{16}$ is completely replaced by the condensed monolayer of $F_{12}H_{16}$. At 2 °C, for example, a surface of H_{14} solution of $F_{12}H_{16}$ covered with a gaseous film of $F_{12}H_{16}$ is replaced by a condensed H_{14} monolayer containing an almost gaseous state of $F_{12}H_{16}$, and is then completely replaced by the condensed monolayer of $F_{12}H_{16}$ with increasing bulk concentration. Above the temperature of the triple point for the $F_{12}H_{16}$ monolayer, the $F_{12}H_{16}$-H_{14} system exhibits a gaseous, expanded, and condensed state.

Keywords Surface crystallization · Semi-fluorinated alkane · Surface hetero-azeotrope · Surface phase transition · Surface tension

Introduction

Recently, several pure liquid interfaces and surfaces have been investigated by measuring their interfacial tension, synchrotron X-ray reflectivity, surface vibrational spectroscopy, and ellipsometry. Also the new phase transition at the interfaces of a long chain liquid alcohol against water and long chain liquid alkane against air has been reported [1, 2, 3, 4, 5, 6, 7, 8]. The phase transition of a thin film of a long chain alkane on a substrate has been studied by differential thermal analysis and ultraviolet photoemission [9]. The phase transition is called surface crystallization or surface freezing. Generally, this type of phase transition occurs at typically a few Kelvins above the bulk freezing point of the material. At the lower temperature, long chain liquid alcohols and long chain liquid alkanes form condensed films at their surfaces. This surface

crystallization has been observed for n-alkanes with the chain length $n \geq 15$ [1, 3, 4, 5, 6, 7, 8, 9].

Semi-fluorinated alkanes of the general diblock structure $F(CF_2)_n(CH_2)_mH$ (abbreviated F_nH_m) have attracted attention in recent years as an innovative model amphiphile for hydrocarbon and fluorocarbon systems [10, 11, 12, 13, 14, 15]. Binks et al reported a phase transition from an expanded state to a highly condensed state of F_{12} H_{14} on the surface of a pentadecane solution [15].

We have previously reported the result of a study on the $F_{12}H_{16}$-H_{16} system [16]. The surface of liquid H_{16} forms a condensed film at 17.64 °C. The condensed monolayer of the $F_{12}H_{16}$ molecule is effectively insoluble in this H_{16} condensed monolayer. Due to the immiscibility of $F_{12}H_{16}$ with the H_{16} condensed film, the $F_{12}H_{16}$-H_{16} system exhibits a surface hetero-azeotrope behavior at about 17.4 °C and shows gaseous, expanded, and condensed monolayer phases above the triple point for the $F_{12}H_{16}$ monolayer.

After the report Gang et al. examined the surface crystallization behavior of the liquid semi-fluorinated alkanes $F_{12}H_{8,}$ $F_{12}H_{14,}$ and $F_{12}H_{19}$ by X-ray and surface tension measurements [17]. They measured the surface tension with the temperature scanning. The present authors usually measure the equilibrium surface tension at a series of temperatures by changing temperature in discrete steps while confirming the establishment of surface tension constancy. They concluded that the semi-fluorinated alkane monolayer of $F_{12}H_8$ and $F_{12}H_{14}$ is crystalline while smectic-like for $F_{12}H_{19}$. They inferred that the crossover between the two behaviors occurs for $F_{12}H_{16}$.

Recently, Marczuk et al measured the X-ray reflectivity of the $F_{12}H_m$-H_n (m = 12, 14, 16, 18, n= 12,16) system and reported that the transition from the gaseous to condensed state is very likely to be continuous in the $F_{12}H_{16}$-H_{16} system [18]. Although two reports pointed out the anomalous behavior of $F_{12}H_{16}$, the $F_{12}H_{16}$-H_{16} system very frequently exhibits a supercooled gaseous state, as mentioned in a previous paper [16]. To obtain reasonable surface tension data for the expanded state, measurement via the condensed state was indispensable. The question concerning the $F_{12}H_{16}$-H_{16} system will be dealt with in a subsequent paper using an additional surface tension measurement and a complementary experimental technique, such as imaging [19] or scattering [17, 18, 20]. It seems that a concordant result from these different measurements will be attained by careful temperature control not only for the constancy but also the history of the measured temperature without any bulk freezing to attain a true equilibrium.

In this paper, H_{14} was used as the solvent because its freezing temperature is not very low (about 6 °C). The motivation for the present study is to investigate the interplay of the surface behavior of pure H_{14}, having no surface crystallization by itself, with $F_{12}H_{16}$. We measured the surface tension of H_{14} solutions of $F_{12}H_{16}$ as a function of temperature and concentration.

Experimental

Materials

1-(Perfluorododecyl)hexadecane, $F_{12}H_{16}$, synthesized according to the method of Rabolt et al [10], was provided by Prof. M. Möller of the University of Ulm, Germany. The product, sublimated for 48 hr after both its synthesis and recrystallization, had a purity of more than 99.3% according to GLC. Tetradecane (Tokyo Kasei, > 99%) was purified using an activated alumina column. The purity of the product was more than 99.6%.

Method

Surface tension measurements were made by the pendant drop technique and calculated by the selected plane method [21]. The drops were suspended from a glass rod to avoid the disturbing influences generally caused by a capillary [22]. An exact location of the pendant drop boundary was detected through optically flat windows of a closed glass cell by a silicon photodiode sensor under a microscope with a magnification of 100 . Exact diameters at an equatorial and a selected plane for the drop were directly measured by a micrometer with a built-in photoelectric rotary encoder within an error of 0.2 μm. The accuracy of this micrometer for this experiment nearly corresponds to that of a video image analysis using a digital camera equipped with 100 million pixels. Thus the precision of the surface tension measurements was ± 0.02 mN m^{-1} in most of the runs. The temperature was controlled within 0.01 K.

Results and discussion

We may choose three intensive variables as the experimental variables to describe this three-component two-phase system by considering Gibbs' phase rule and postulating that the air is one component. We employed the molality of $F_{12}H_{16}$, m_1, and temperature, together with pressure. We measured the surface tension γ of a H_{14} solution by lowering the temperature in discrete steps, with an equilibration time of up to 1 hr at each experimental temperature at a constant molality m_1 of $F_{12}H_{16}$ in the temperature range from 2 °C to 40 °C under atmospheric pressure.

The surface tension values are plotted versus temperature in Fig. 1. All curves were described by fitting two linear and polynomial function to the experimental results. In this figure, the γ vs T curve for pure H_{14} shows good linearity and no break point. We measured the surface tension for pure H_{14} down to the freezing temperature for the pendant drop at about 2.5 °C, while the bulk freezing point is about 6 °C. The curves of the three most diluted H_{14} solutions of $F_{12}H_{16}$ (m_1 < 0.49 mmol kg^{-1}) have a break point at lower temperatures and consist of two nearly linear sections, with

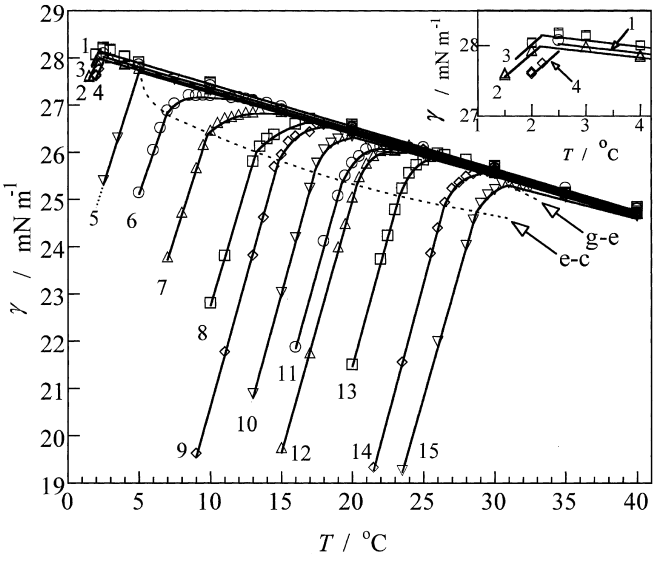

Fig. 1 Surface tension vs temperature curves at constant molality for m_1: (1) 0 mmol kg^{-1}, (2) 0.101, (3) 0.199, (4) 0.299, (5) 0.486, (6) 0.628, (7) 0.828, (8) 1.196, (9) 1.501, (10) 1.965, (11) 2.461, (12) 2.947, (13) 3.937, (14) 5.939, and (15) 7.011

$(\partial\gamma/\partial T)_{p,m_1} > 0$ at a low temperature and $(\partial\gamma/\partial T)_{p,m_1} < 0$ at a high temperature.

At the higher concentrations of $F_{12}H_{16}$, the curves in this figure suggest three distinct regions. In the higher surface tension region, the slope of the curve is again negative and independent of temperature and concentration. In the lower surface tension region, the curves are again nearly linear with a large positive slope that is almost independent of the concentration. In contrast to this linear dependence of γ on T and m_1 in the higher and lower surface tension regions, the value of the slope in the intermediate region indicates a pronounced increase with increasing molality and temperature. Therefore the dashed lines in Fig. 1 describe the loci of the two borderlines among the three regions. The derivative $(\partial\gamma/\partial T)_{p,m_1}$ of the γ vs T curves discontinuously change at the border of the different sections. As will be explained later, these borderlines signify the loci of the first order surface phase transitions of the system. Further, we can notice the difference in stabilities of the lower surface tension region (the temperature range of the existence of the state below the break point at lower temperature) between the three most diluted solutions and the others in Fig. 1.

The precise surface tension measurement reveals the notable dynamic surface phenomenon of the $F_{12}H_{16}$-H_{14} system. While in the high and low-temperature regions the surface tension of a given pendant drop was fully reversible in the cooling-heating cycles, systematic effects of the supercooling phenomenon on the surface tension were observed very often in the intermediate region. Also, an almost constant or a slight increasing surface tension with decreasing temperature at a constant concentration of $F_{12}H_{16}$ indicating gel formation [10, 11, 14, 23] was observed in the solution at concentrations above about 0.8 mmol kg^{-1}. The gel is thought to consist of a network of highly anisometric (needle-like) crystallites of $F_{12}H_{16}$ with entrapped solvent [23, 24]. All such behavior is very similar to that of the previously reported $F_{12}H_{16}$-H_{16} system [16]. All values influenced by the supercooling phenomenon and by gel formation were omitted in Fig. 1.

Adopting the two dividing planes convention [25, 26, 27], we considered the entropy change associated with the adsorption Δs defined by

$$\Delta s = s^{\mathrm{H}} - \Gamma_1^{\mathrm{H}} s_1 \tag{1}$$

and calculated it using

$$\Delta s = -(\partial\gamma/\partial T)_{p,m_1} \tag{2}$$

where s^{H} is the surface excess entropy per unit area and s_1 is the partial molar entropy of $F_{12}H_{16}$ in the H_{14} solution. The values of Δs at several temperatures are plotted versus m_1 in Fig. 2. At first glance, we notice that there are four distinct regions. The discontinuities in the isotherms show that all the surface phase transitions in this system may be considered to be of first order within the framework of surface tension measurement and its thermodynamic analysis.

To show the concentration dependence of the surface tension, the values of γ at the given temperatures and on the borderlines were read from Fig. 1 and plotted versus molality in Fig. 3. The values for the pure H_{14} and the solution of m_1 = 0.486 mmol kg^{-1} at 2 °C in Fig. 2 were

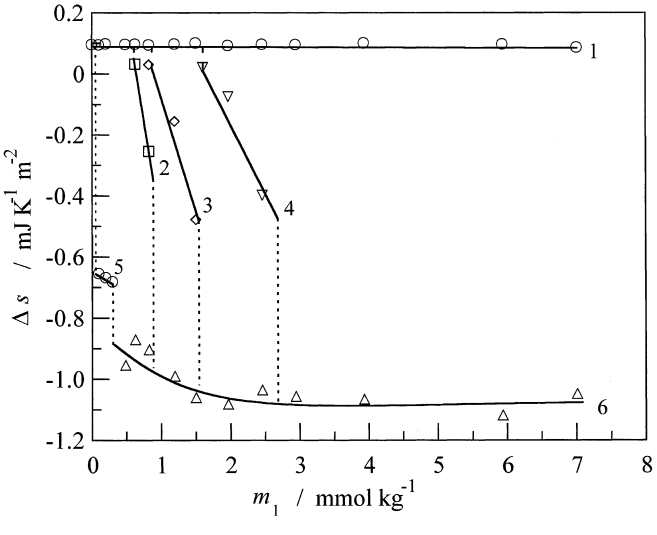

Fig. 2 Entropy change vs molality curves at constant temperature: (1) gaseous state in the range of about 2.00 to 40.00 °C, expanded state at (2) 10.00 °C, (3) 15.00 °C, (4) 20.00 °C, (5) condensed state mainly composed of H_{14} at 2.00 °C, and (6) condensed state mainly composed of $F_{12}H_{16}$ in the range of about 2.00 to 25.00 °C

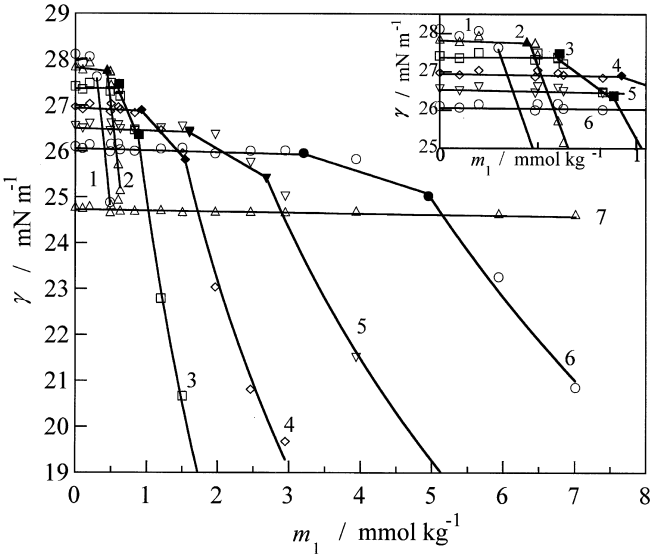

Fig. 3 Surface tension vs molality curves at constant temperature: (1) 2.00 °C, (2) 5.00, (3) 10.00, (4) 15.00, (5) 20.00, (6) 25.00, and (7) 40.00; closed symbols indicate the values on the dashed lines in Fig. 1

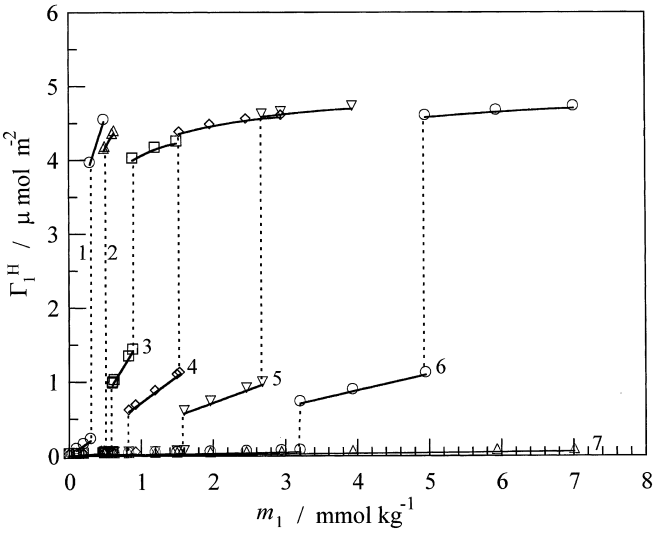

Fig. 4 Surface density of $F_{12}H_{16}$ vs molality curves at constant temperature: (1) 2.00 °C, (2) 5.00, (3) 10.00, (4) 15.00, (5) 20.00, (6) 25.00, and (7) 40.00

given by using an extrapolation of the straight line in Fig. 1. The surface phase transitions are distinguished by pronounced discontinuities in the slope of the isotherms. As expected from Figs. 1 and 2, only one surface phase transition occurs near to 5 °C, while two types of phase transitions occur above and below that temperature. Concerning the phase transition below that temperature, however, we could not draw the lines at lower concentrations ($m_1 < 0.30$ mmol kg^{-1}, namely curve 1) due to rather smaller changes than the experimental error in the surface tension. We only plotted the surface tension values with the error limits described by the size of each symbol at 2 °C in Fig. 3. Nevertheless, we should point out the existence of two types of phase transitions at 2 °C as can be seen in Fig. 2. At 40 °C, no phase transition occurs within the experimental concentration range.

Next, we evaluate the surface density Γ_1^H of $F_{12}H_{16}$ by using

$$\Gamma_1^H = -(m_1/RT)(\partial\gamma/\partial m_1)_{T,p} \quad (3)$$

where the subscript p is the pressure that we used as the atmospheric pressure for the experimental variable [25]. The $F_{12}H_{16}$ solution was assumed to exhibit ideal behavior in this experimental range [15]. All curves in Fig. 3 were described by a fitting of the formula for the Frumkin isotherm to the experimental result [16], except in the low concentration region where γ is a linear function of m_1.

The evaluated Γ_1^H values at constant temperature are plotted versus m_1 in Fig. 4. The remarkable steps in these adsorption isotherms reflect the discontinuity in the slope at the break points of the curves in Fig. 3. In view of the largest value of the surface density, and the maximum bulk concentration, $F_{12}H_{16}$ can be regarded as the surface-active solute at the air/ H_{14} solution interface and more surface-active at the air/ H_{16} solution interface [16]. This tendency agrees with that reported by Binks et al [15].

To view such a behavior more clearly, we calculated the surface pressure π and the mean area per adsorbed molecule A, respectively, by equations

$$\pi = \gamma^0 - \gamma \quad (4)$$

and

$$A = 1/N_A\Gamma_1^H \quad (5)$$

where γ^0 is the surface tension of the free surface of pure H_{14} and N_A is Avogadro's constant. We compared the π vs A curves of the present $F_{12}H_{16}$-H_{14} system with that of the $F_{12}H_{16}$-H_{16} system, fluorododecanol $F(CF_2)_{10}(CH_2)_2OH$ (abbreviated $FC_{12}OH$), and 1-octadecanol (abbreviated $C_{18}OH$) at the hexane/water interface in Fig. 5a. It has been established in the studies of these substances that an adsorbed film of $C_{18}OH$ transfers from the expanded to the condensed state, while that of $FC_{12}OH$ transfers from the gaseous to the condensed state [28, 29].

For the smaller area in Fig. 5a, the isotherm of the $F_{12}H_{16}$-H_{14} system (curve 1) bears a close resemblance to that of the $F_{12}H_{16}$-H_{16} system (curve 2) and of $FC_{12}OH$ (curve 3) in the condensed state. For the intermediate area, the shape of the curve for the $F_{12}H_{16}$-H_{14} system (curve 1) resembles that of $C_{18}OH$ (curve 4)

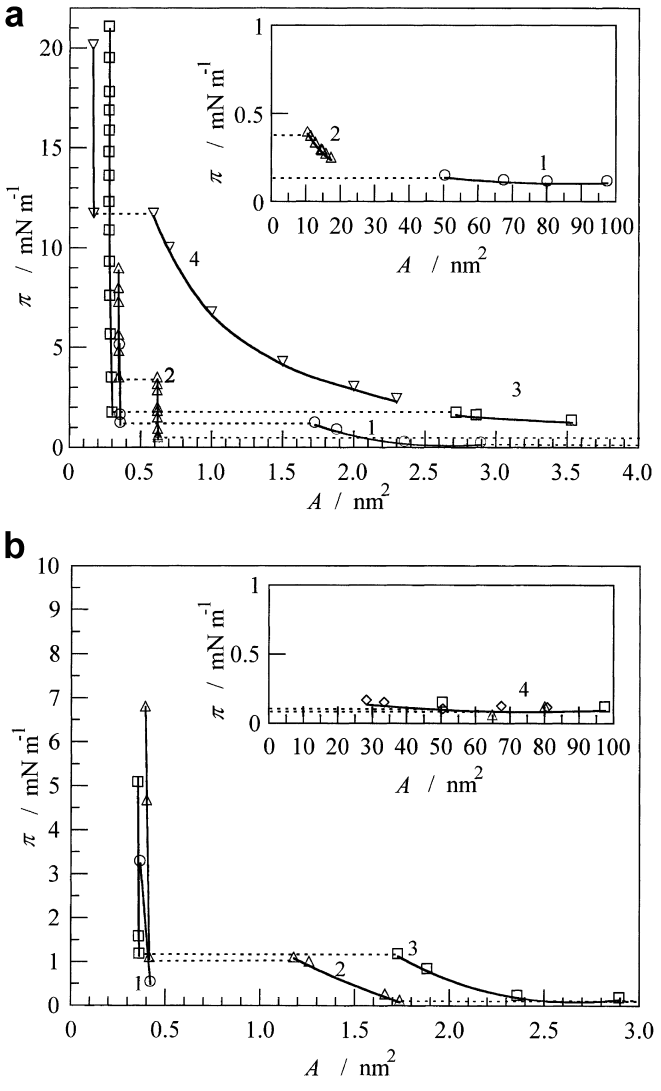

Fig. 5 Surface pressure vs mean area per molecule curves at constant temperature: **a**: (1) $F_{12}H_{16}$ - H_{14} system at 20.00 °C, (2) $F_{12}H_{16}$ - H_{16} system at 24.00 °C, (3) $FC_{12}OH$ at hexane/water system at 25.00 °C, (4) $C_{18}OH$ at hexane/water system at 25.00 °C; **b**: (1) $F_{12}H_{16}$ - H_{14} system at 2.00 °C, (2) 10.00 °C, (3) 20.00 °C, (4) 5.00 ~ 40.00 °C

in the expanded state though the values of π for the $F_{12}H_{16}$-H_{14} system are too small. Furthermore, the π vs A isotherm of the $F_{12}H_{16}$-H_{14} system (curve 1) for the larger area is similar to that of the $F_{12}H_{16}$-H_{16} system (curve 2) in the gaseous state. These similarities with the behavior of the $FC_{12}OH$, $C_{18}OH$, and $F_{12}H_{16}$ in H_{16} systems support our description that the adsorbed monolayer of the $F_{12}H_{16}$ in H_{14} system reveals gaseous, expanded, and condensed states.

According to these assignments of each state, we consider the entropy change of these states in Fig. 2 in more detail. The value of the entropy change in the gaseous state is almost constant and the same as that of the pure H_{14} surface. The Δs value in the expanded film rapidly decreases with an increase in m_1. In the condensed state, the value of Δs gradually decreases with increasing m_1 and attains a nearly constant value. In the lower concentration region at 2 °C there is another entropy state between the gaseous and condensed states. It resulted from the positive slope of the curves of the three most diluted H_{14} solutions of $F_{12}H_{16}$ ($m_1 < 0.30$ mmol kg^{-1}) at lower temperature below a break point in Fig. 1. The magnitude and sign of the Δs value in the state signify a restricted structure at the surface and shows that the state is supposed to be a condensed one. The value of Δs in the state, about - 0.7 mJ K^{-1} m^{-2}, is slightly greater than that of the pure condensed H_{16} state in the $F_{12}H_{16}$-H_{16} system previously studied [16].

Fig. 5b provides a detailed explanation about the π vs A curves of the $F_{12}H_{16}$-H_{14} system at several temperatures. The π vs A curves of the $F_{12}H_{16}$-H_{14} system at 10 °C (curve 2) and 20 °C (curve 3) exhibit the usual gaseous, expanded, and condensed states. As we have already described in the explanation for Figs. 2 and 3, there are two types of phase transitions at 2 °C and the Γ_1^H value of $F_{12}H_{16}$ at lower concentrations ($m_1 < 0.30$ mmol kg^{-1}) could not be calculated. It is supposed to be very small, such that the two types of the phases are almost gaseous states of the $F_{12}H_{16}$ monolayer at the H_{14} surface. From Eqn. 5, for the definition of the molecular area, however, it is clear that the value of the molecular area is no more than the area per $F_{12}H_{16}$ molecule irrespective of other species existing in the surface.

Judging from Figs. 1, 2, and 3, we can describe the surface of the H_{14} solutions of $F_{12}H_{16}$ at lower concentrations ($m_1 < 0.30$ mmol kg^{-1}) and at lower temperature ($T < 3$ °C) as the condensed film mainly composed of H_{14} molecules. Therefore the condensed H_{14} state is a condensed state of almost a pure H_{14} monolayer with a very small number of $F_{12}H_{16}$ molecules such that its extent implies a gaseous state in the usual case. It is clear from Fig. 1 that the pure liquid H_{14} freezes without forming a condensed film at its surface in this experimental condition. Therefore, it is worth noting that a very small amount of $F_{12}H_{16}$ initiates the formation of the condensed H_{14} surface film. In other words, a small amount of $F_{12}H_{16}$ molecules play an important role to enhance the interaction and orientation between the H_{14} molecules so as to attain the condensed state.

Next, Fig. 6 shows the schematic surface tension vs temperature diagrams corresponding to a generic surface phase diagram for two different systems. Fig. 6a, the diagram for the $F_{12}H_{16}$-H_{16} system, represents the case of complete immiscibility of $F_{12}H_{16}$ with the condensed monolayer of H_{16}. The immiscibility of the $F_{12}H_{16}$ molecule with that of H_{16} in the

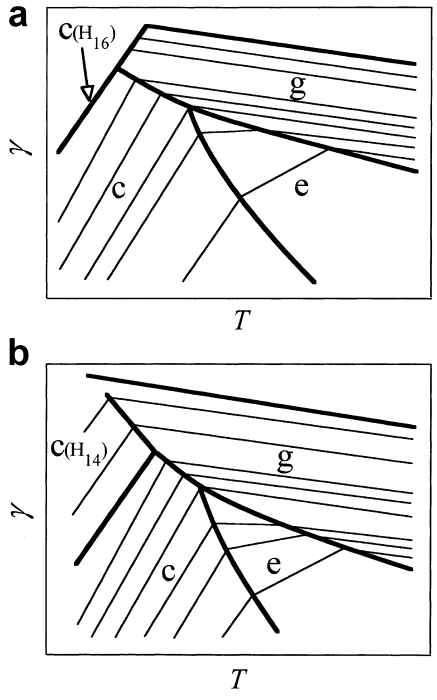

Fig. 6 Schematic surface tension vs temperature curves at constant molality for **a** $F_{12}H_{16}$ - H_{16} system, **b** $F_{12}H_{16}$ - H_{14} system. **g** denotes gaseous state, **e** expanded state, **c** condensed state, ($C_{(H_{16})}$) condensed state of H_{16}, ($C_{(H_{14})}$) condensed state of H_{14}

condensed state make the system have a surface hetero-azeotrope behavior at a temperature slightly below the surface freezing point of H_{16}. The $F_{12}H_{16}$-H_{16} system exhibits also the gaseous, expanded, and condensed states above the triple point for the $F_{12}H_{16}$ monolayer.

In contrast to the $F_{12}H_{16}$-H_{16} system, Fig. 6b for the $F_{12}H_{16}$-H_{14} system shows that the condensed monolayer of H_{14} has a finite solubility of $F_{12}H_{16}$. It seems that the interaction both between the H_{14} molecule and the H_{16} chain of the $F_{12}H_{16}$ molecule and between the F_{12} chains of the $F_{12}H_{16}$ molecules forces the H_{14} molecules to form an oriented close-packed structure. After increasing the bulk concentration of $F_{12}H_{16}$, the F_{12} chains of the $F_{12}H_{16}$ molecules form a close-packed film in another condensed state. Hence, as in the case of the H_{16} system, the H_{14} system also exhibits a surface hetero-azeotrope behavior in the lower temperature region. There is no significant surface density of $F_{12}H_{16}$ in the frozen monolayer of H_{16} in the $F_{12}H_{16}$-H_{16} system. Therefore, the phase transition at lower temperature corresponds to a complete displacement of a monolayer of condensed H_{16} by a condensed monolayer of $F_{12}H_{16}$. Also, at the lower temperature in the $F_{12}H_{16}$-H_{14} system, the condensed H_{14} monolayer containing a very small amount of $F_{12}H_{16}$ is completely replaced by the condensed monolayer of $F_{12}H_{16}$. At 2 °C, for example, a surface of H_{14} solution of $F_{12}H_{16}$ covered with a gaseous film of $F_{12}H_{16}$ is replaced by a condensed H_{14} monolayer containing almost a gaseous state of $F_{12}H_{16}$ which is then completely replaced by the condensed monolayer of $F_{12}H_{16}$ with increasing m_1.

To examine the place of a locus of the first order surface phase transition from a condensed H_{14} monolayer to a condensed $F_{12}H_{16}$ monolayer (bold line between the region of $C_{(H_{14})}$ and C in Fig. 6b) in Fig. 1, we suppose the condensed film in the $F_{12}H_{16}$-H_{14} system to be comprised of two phases, α and β, in equilibrium. We can describe the thermodynamic quantities in each phase by the relations

$$d\gamma = -\Delta s^{\alpha} dT + \Delta v^{\alpha} dp - \Gamma_1^{H,\alpha}(\partial\mu_1/\partial m_1)_{T,p} dm_1 \tag{6}$$

and

$$d\gamma = -\Delta s^{\beta} dT + \Delta v^{\beta} dp - \Gamma_1^{H,\beta}(\partial\mu_1/\partial m_1)_{T,p} dm_1, \tag{7}$$

where the superscripts α and β indicate the phases α and β, respectively. Eliminating the variable m_1 between Eqns. 6 and 7 at constant pressure, we then obtain

$$(\partial\gamma^{\mathrm{eq}}/\partial T)_p = -\left(\Delta s^{\beta}\Big/\Gamma_1^{H,\beta} - \Delta s^{\alpha}\Big/\Gamma_1^{H,\alpha}\right)\Big/\left(1\Big/\Gamma_1^{H,\beta} - 1\Big/\Gamma_1^{H,\alpha}\right), \tag{8}$$

where superscript eq means that the two phases coexist in equilibrium. Upon substituting the numerical values $\Delta s^{C_{H_{14}}} = -0.690\,\mathrm{mJ\,K^{-1}\,m^{-2}}$, $\Delta s^{F_{12}H_{16}} = -0.894\,\mathrm{mJ\,K^{-1}\,m^{-2}}$, and $\Gamma_1^{H,C_{F_{12}H_{16}}} = 3.94\ \mu\mathrm{mol\,m^{-2}}$ evaluated from Figs. 2 and 4, and supposed value $\Gamma_1^{H,C_{H_{14}}} = 0.20\ \mu\mathrm{mol\,m^{-2}}$ at 2 °C, we can evaluate the slope of the surface tension of the break point vs temperature curve. We then obtain

$$-(\partial\gamma^{\mathrm{eq}}/\partial T)_p = -0.679 \pm 0.019\,\mathrm{mN\,m^{-1}\,K^{-1}}$$

which is just slightly greater than the value of $\Delta s^{C_{H_{14}}}$. Therefore, this estimation predicts that if the $m_1 =$ 0.299 mmol kg^{-1} H_{14} solution of $F_{12}H_{16}$, for example, is not frozen down to a lower temperature than 2 °C, then a break point for the phase transition from a condensed H_{14} monolayer to a condensed $F_{12}H_{16}$ monolayer on the γ vs T curve can be observed at about 2 °C in Fig. 1.

Here, we consider the energy change associated with the adsorption Δu given by

$$\Delta u = \gamma + T\Delta s - p\Delta v. \tag{9}$$

Because the $p\Delta v$ term on the right-hand side is negligibly small compared to the other terms under atmo-

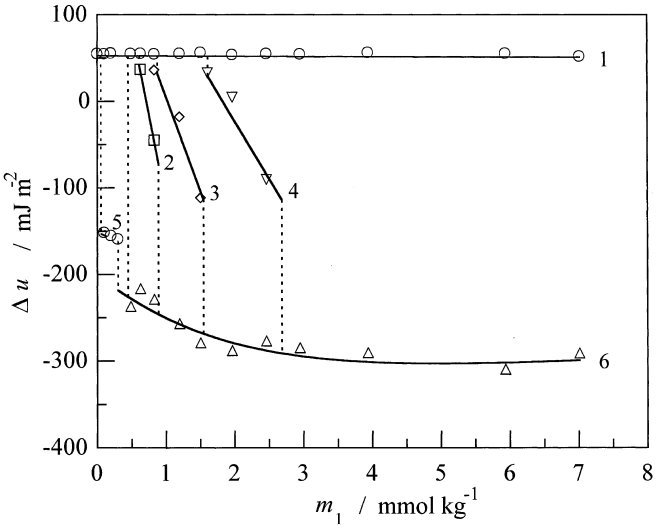

Fig. 7 Energy change vs molality curves at constant temperature: (1) gaseous state in the range of about 2.00 to 40.00 °C, expanded state at (2) 10.00 °C, (3) 15.00 °C, (4) 20.00 °C, (5) condensed state mainly composed of H_{14} at 2.00 °C, and (6) condensed state mainly composed of $F_{12}H_{16}$ in the range of about 2.00 to 25.00 °C

spheric pressure [30], the value of Δu is evaluated by making use of Figs. 2 and 5, and plotted versus m_1 in Fig. 7. In the thermodynamic sense, the interaction produces a significant decrease in the entropy change. Also the disadvantage of the decrease in the entropy change is compensated by the significant decrease in the energy change. It is important to understand that the condensed H_{14} state cannot exist in the pure H_{14} system and that its appearance is caused by the interaction both between the H_{14} molecule and the H_{16} chain of the $F_{12}H_{16}$ molecule and between the F_{12} chains of the $F_{12}H_{16}$ molecules. To estimate the effect of the interaction between the F_{12} chains of the $F_{12}H_{16}$ molecules on the appearance of the condensed H_{14} state, a detailed investigation of the H_{16}-H_{14} system and comparison of the behavior with that of the present system at low temperature will be undertaken.

Acknowledgements This work was supported by research grants from Chikushi Jogakuen Junior College.

References

1. Earnshaw JC, Hughes C (1992) J Phys Rev A 46:R4494
2. Aratono M, Takiue T, Ikeda N, Nakamura A, Motomura K (1993) J Phys Chem 97:5141
3. Wu XZ, Ocko BM, Sirota EB, Sinha SK, Deutsch M, Cao BH, Kim MW (1993) Science 261:1018
4. Wu XZ, Sirota EB, Sinha SK, Ocko BM, Deutsch M (1993) Phys Rev Lett 70:958
5. Sefler GA, Du Q, Miranda PB, Shen YR (1995) Chem Phys Lett 235:347
6. Pfohl T, Beaglehole D, Riegler H (1996) Chem Phys Lett 260:82
7. Doerr A, Wu XZ, Ocko BM, Sirota EB, Gang O, Deutsch M (1997) Colloids Surf A 128:63
8. Ocko BM, Wu XZ, Sirota EB, Sinha SK, Gang O, Deutsch M (1997) Phys Rev E 55:3164
9. Yamamoto Y, Ohara H, Kajikawa K, Ishii H, Ueno N, Seki K, Ouchi Y (1999) Chem Phys Lett 304:231
10. Twieg RJ, Russell TP, Siemens R, Rabolt JF (1985) Macromolecules 18:1361
11. Höpken J, Pugh C, Richtering W, Mšller M (1988) Makromol Chem 189:911
12. Turberg MP, Brady JE (1988) J Am Chem Soc 110:7797
13. Lo Nostro P, Chen S-H (1993) J Phys Chem 97:6535
14. Gaines GLJr (1991) Langmuir 7:3054
15. Binks BP, Fletcher PDI, Sager WFC, Thompson RL (1995) Langmuir 11:977
16. Hayami Y, Findenegg GH (1997) Langmuir 13:4865
17. Gang O, Ellmann J, Möller M, Kraack H, Sirota EB, Ocko BM, Deutsch M (2000) J Europhys Lett 49:761
18. Marczuk P, Lang P, Findenegg GH, Mehta SK, Möller M (2002) Langmuir 18:6830
19. Mckenna CE, Knock MM, Bain CD (2000) Langmuir 16:5853
20. Zhang Z, Mitrinovic DM, Williams SM, Huang Z, Schlossman ML (1999) J Chem Phys 110:7421
21. Andreas JM, Hauser EA, Tucker WB (1938) J Phys Chem 42:1001
22. Hayami Y (1996) Colloid Polym Sci 274:643
23. Höpken J (1991) PhD thesis. University of Twente, The Netherlands
24. Lo Nostro P (1995) Adv Colloid Interface Sci 56:245
25. Motomura K (1978) J Colloid Interface Sci 64:348
26. Motomura K, Aratono M (1987) Langmuir 3:304
27. Hansen RS (1962) J Phys Chem 66:410
28. Matubayasi N, Motomura K, Aratono M, Matuura R (1978) Bull Chem Soc Jpn 51:2800
29. Hayami Y, Uemura A, Ikeda N, Aratono M, Motomura K (1995) J Colloid Interface Sci 172:142
30. Motomura K, Iwanaga S, Hayami Y, Uryu S, Matuura R (1981) J Colloid Interface Sci 80:32